Electronic Supplementary Material (ESI) for Journal of Materials Chemistry A.

Supporting information

Holmium Rare Earth Metal Ion Incorporated and Ambient-Air Processed All-Inorganic γ-$CsPbI_{2.5}Br_{0.5}$ Perovskite Solar Cells Yielding High Efficiency and Stable Performance

Jyoti V. Patil, [a, b] **Sawanta S. Mali,** [b] **Chang Kook Hong** [a, b*]

[a]*Optoelectronic Convergence Research Center, School of Chemical Engineering, Chonnam National University, Gwangju, 61186, South Korea.*

[b]*Polymer Energy Materials Laboratory, School of Chemical Engineering, Chonnam National University, Gwangju, 61186, South Korea.*

***Corresponding author**: hongck@chonnam.ac.kr

S1: Details of all chemicals

The chemical including cesium iodide (CsI) (Sigma, 99.999 %), lead bromide ($PbBr_2$) (Sigma, ≥98%), lead iodide (PbI_2) (Sigma, 99%), holmium (III) chloride ($HoCl_3$) (Sigma, 99.99%), (Sigma, 99.99%), dimethyl sulfoxide (DMSO), (N, N-dimethylformamide (DMF), poly(3-hexylthiophene-2,5-diyl) (P3HT) (Sigma-Aldrich, average Mw 50,000-100,000) were purchased from Sigma-Aldrich. For the hot-air source, a BOSCH GHG 630 DCE Hot Air Gun - 0601 94C 740 was used.

S2: Details of experimental procedure of IPVSCs device fabrication

Fluorine-doped tin oxide (FTO) coated substrates were ultrasonically cleaned by following the sequence of detergent, distilled water and ethanol for 15 min for each step and treated with UV plasma for 10 min. The compact-TiO_2 (c-TiO_2), mesoporous TiO_2 (mp-TiO_2), $TiCl_4$ treatment were prepared by following a similar process that we reported earlier [S1, S2]. For the preparation of a perovskite precursor solution with a concentration of 1.2 M $CsPb(I_{1-n}Br_n)_3$, the following materials were stoichiometrically mixed in 1 ml of anhydrous DMSO: 0.415 g of PbI_2, 0.110 g of $PbBr_2$, 0.312 g of CsI and 1.2 M DMAI. This resulting solution was stirred at a temperature of 75 °C for an overnight period. Moreover, a stock solution of holmium (III) chloride ($HoCl_3$) was precisely prepared using a combination of DMSO and DMF solvents in a 1 : 2 ratio. The γ-$CsPbI_{2.5}Br_{0.5}$-based perovskite films were synthesized via the addition of the various amounts of the $HoCl_3$ from 0 to 4% into the aove perovskite solution. The resulting films were designated as follows: γ-$CsPbI_{2.5}Br_{0.5}$, 1 % $HoCl_3$, 2 % $HoCl_3$, 3 % $HoCl_3$ and 4 % $HoCl_3$-based perovskite representing a series of perovskite thin films. To balance perovskite composition, an equivalent quantity of CsBr (1.2 M in formamide) was exactly introduced into the precursor solution. Subsequently, this perovskite solution was spun at two-stage spinning process: firstly, at 1000 rpm for 10 seconds, followed by a second stage at 3000 rpm for 30 seconds. During spinning stage at 3000 rpm, a flow of hot air was applied onto the spinning substrate for 10 seconds. Later, all films were annealed at 220 °C for 5 min. To prepare a (P3HT solution) hole-transporting layer (HTL) and a gold (Au) deposition by thermal evaporation to complete the IPVSCs, we followed our previous reports [S3, S4].

S3: Details of various characterization techniques

Surface morphology images were captured by utilizing a scanning electron microscope (SEM; S-4700, Hitachi). X-ray diffraction (XRD) analyses were conducted by employing a

D/MAX Ultima III-XRD spectrometer (PANalytical, Japan) equipped with a Cu Kα line of 1.5410 Å. Optical absorption measurements were carried out on a UV-vis spectrophotometer (Varian, CARY, 300 Conc.) in the 500-900 nm wavelength range. Elemental analysis was conducted by employing X-ray photoelectron spectroscopy (XPS) using a VG Multilab 2000-Thermo Scientific (USA, K-Alpha) instrument equipped with a multi-channel detector capable of withstanding high photon energies ranging from 0.1 to 3 keV. For energy-dispersive X-ray (EDX) elemental mapping, the scanning transmission electron microscopy (STEM) mode was utilized. Contrast enhancement against the background of the High-Angle Annular Dark-Field Scanning Transmission Electron Microscopy (HAADF-STEM) images was achieved through background selection using the Rois mode at a detector angle of 14.6 degrees. Additionally, depth profile and elemental mapping of the perovskite films were accomplished using a Time-of-Flight Secondary-Ion Mass Spectrometry (ToF-SIMS^5) instrument (ION-TOF GmbH). The ultraviolet-photoelectron spectroscopy (UPS) measurements were carried out using Thermo VG Scientific Sigma Probe, UK, UV Monochromatic He I (21.22 eV) gas, (Bias -5.0 V, Aperture size 8 mm adjustable) for UPS base UHV pressure 1 x 10^{-9} mB without surface treatment.

The IPVSCs were illuminated using a solar simulator at AM 1.5 G for 10 s, where the light intensity was adjusted with an NREL-calibrated Si solar cell with a KG-5 filter to 1 sun intensity (100 mW cm^{-2}). The photovoltaic performance of IPVSC devices were measured by metal shadow masks with active small area of 0.3 x 0.3 =0.09 cm^2. The exact illumination to the active area was fixed via attaching thin metal shadow mask from backside throughout measurements. The *J-V* curves were measured along with the reverse scan direction from 1.5 V to − 0.05 V or the forward scan direction from −0.05 V to 1.5 V. Time-resolved photoluminescence (TRPL) decay transients were measured at 650 nm using excitation with a 470 nm light pulse at a frequency of 5MHz from the Spectrophotometer F-7000.

The spectral response was taken by a spectral IPCE measurements system (K3100, Mc-Science), which was equipped with a monochromator, a K240×E 300 lamp source connected with K401 OLS XE300W lamp power supply and a K102 signal amplifier. Prior to the use of the light intensity were calibrated using a Si-photodiode (Model: S1337-1010BQ) and In GaAs photodiode (model: G12180-050A) for 300-1100 nm and 1100-1400 nm calibration respectively. Measurements were taken in EQE mode. The Nyquist plot was obtained via conducting EIS analysis with the help of Iviumstat (Ivium Technologies B.V., Eindhoven, and the Netherlands) at

an open-circuit potential at frequencies ranging from 10^{-1} to 10 Hz with AC amplitude of 10 mV. For equivalent circuit analysis, Z-view 2.8d was used.

The steady-state efficiencies were obtained by tracking the maximum power point. The IPVSC devices were illuminated using a solar simulator at AM 1.5 G for 10 s, where the light intensity was adjusted with an NREL-calibrated Si solar cell with a KG-5 filter to 1 sun intensity (100 mW cm^{-2}). The device stability was tested in an ambient condition without encapsulation and after each measurements devices were stored in ambient condition without any encapsulation. Devices were kept in petri dish in ambient air without any encapsulation for the long-term stability. Periodic J-V (current-voltage) curves were recorded under simulated AM1.5 G sunlight at room temperature.

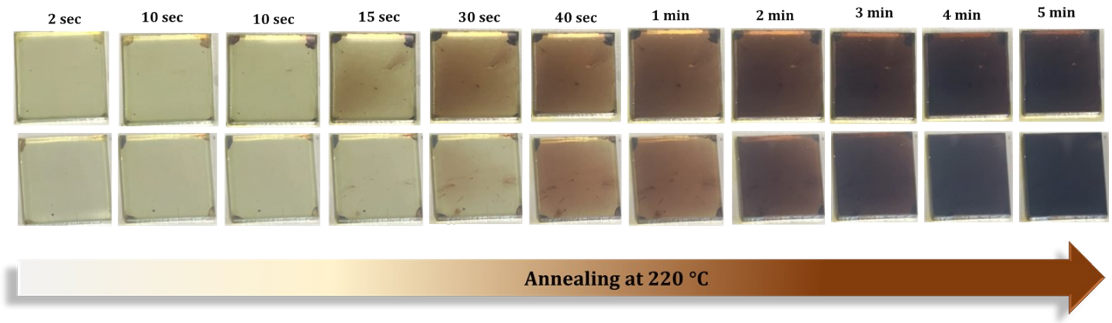

Figure S1. Photographs of the γ-$CsPbI_{2.5}Br_{0.5}$ and 3 % $HoCl_3$-based perovskite during solvent evaporation and crystallization at 220 °C.

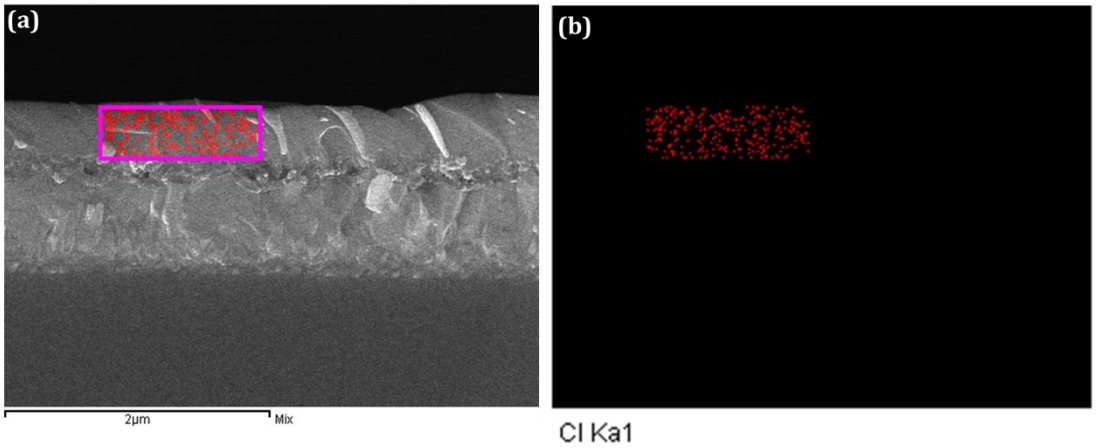

Figure S2: (a) Cross-sectional SEM image of the 3 % $HoCl_3$-based perovskite layer and (b) elemental mapping of the $HoCl_3$ doped γ-$CsPbI_{2.5}Br_{0.5}$-based perovskite layer.

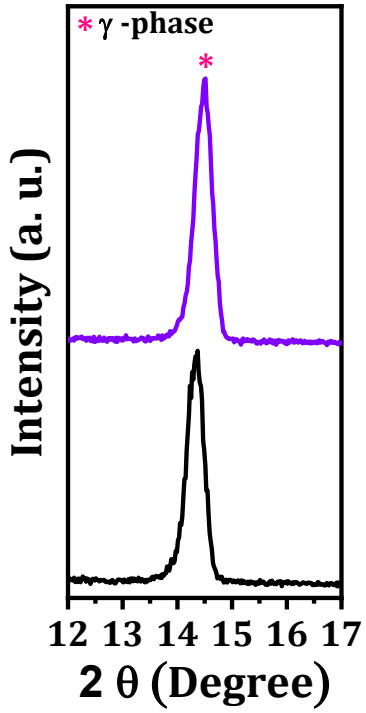

Figure S3: Magnified XRD peaks of the γ-$CsPbI_{2.5}Br_{0.5}$ and 3 % $HoCl_3$-based perovskite thin films.

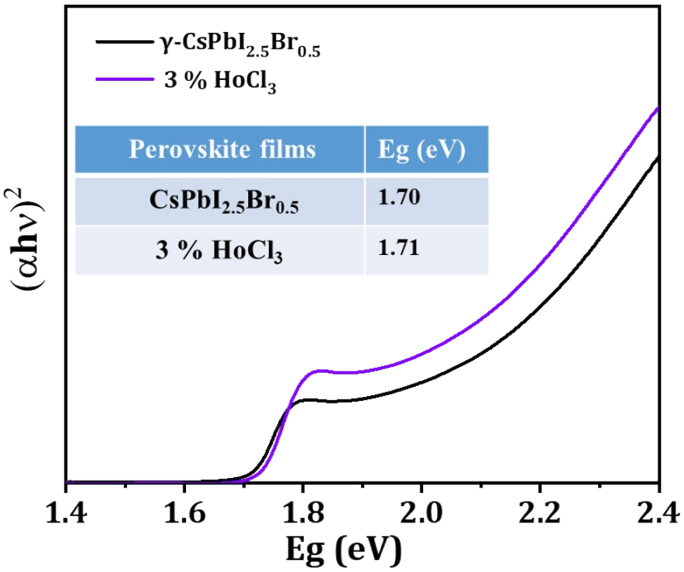

Figure S4: Tauc plots of the γ-$CsPbI_{2.5}Br_{0.5}$ and 3 % $HoCl_3$-based perovskite thin films.

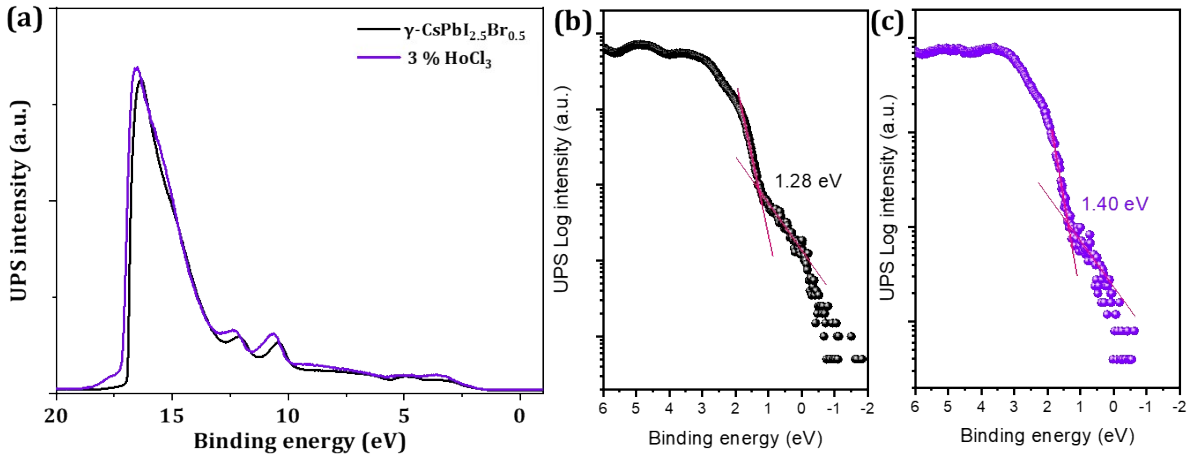

Figure S5: (a) UPS survey spectra of the perovskite films, valance band region of the (b) γ-$CsPbI_{2.5}Br_{0.5}$ and (c) 3 % $HoCl_3$-based perovskite films.

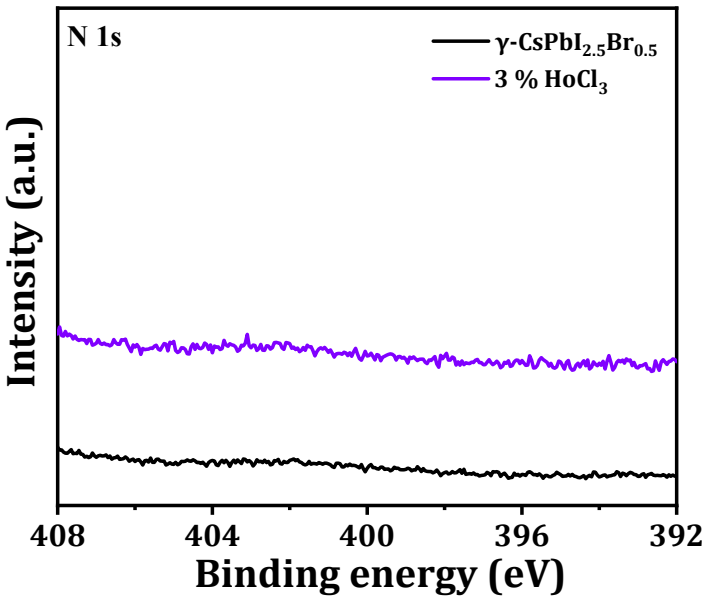

Figure S6: N1S core level of the γ-$CsPbI_{2.5}Br_{0.5}$ and 3 % $HoCl_3$-based perovskite films.

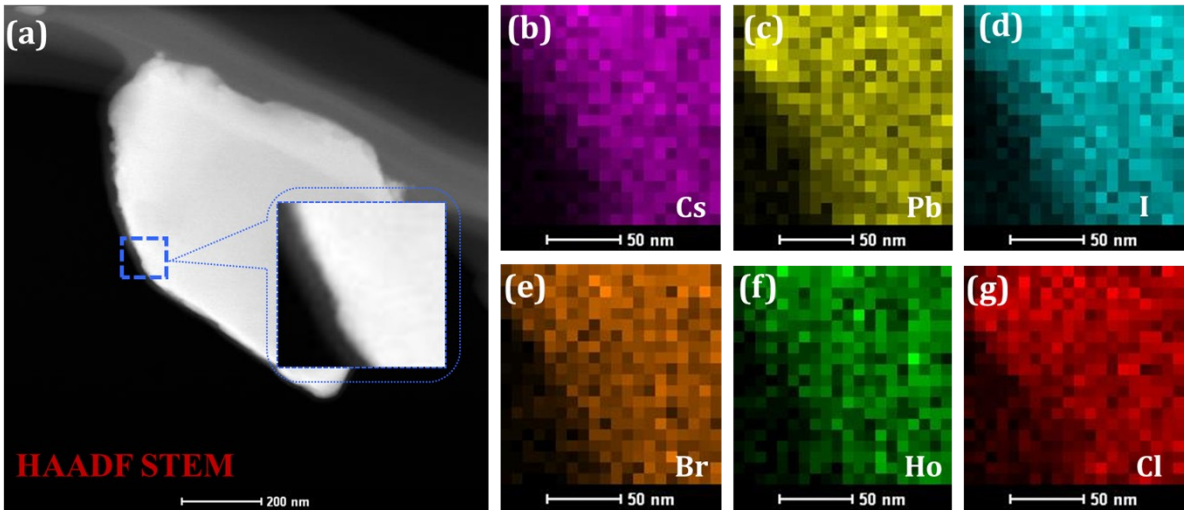

Figure S7: Elemental mapping of the 3 % $HoCl_3$-based perovskite (a) HAADF STEM image, (b) cesium, (c) lead, (d) iodide, (e) bromide, (f) holmium and (g) chloride.

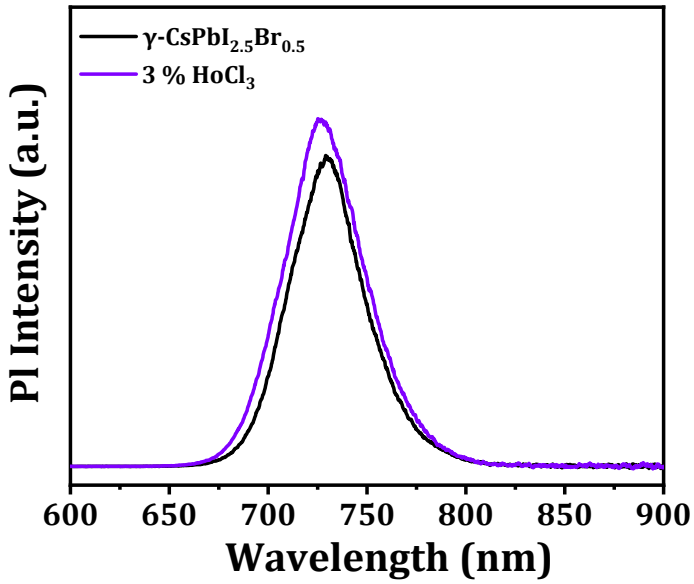

Figure S8: Photoluminescence spectra of the γ-$CsPbI_{2.5}Br_{0.5}$ and 3 % $HoCl_3$-based perovskite thin films.

Table S1: Calculated UPS parameters for energy level of the γ-$CsPbI_{2.5}Br_{0.5}$ and 3 % $HoCl_3$-based perovskite films from UPS spectra.

Samples	E_{cutoff} (eV) (±0.05)	WF (ϕ) (eV)	VBM-E_F (eV) (±0.05)	VBM (eV)	ΔE_g (eV)	CBM (eV)
γ-$CsPbI_{2.5}Br_{0.5}$	16.93	4.29	1.28	5.57	1.70	3.87
3 % $HoCl_3$	17.16	4.06	1.40	5.46	1.71	3.75

Table S2: TRPL measurements of the γ-$CsPbI_{2.5}Br_{0.5}$ and 3 % $HoCl_3$-based perovskite thin films.

Perovskites films	τ_1 **(ns)**	τ_2 **(ns)**	A_1*	A_2*	$<\tau_{avg}>$ **(ns)**
γ-$CsPbI_{2.5}Br_{0.5}$	2.2	0.76	4.29	1.5	1.49
3 % $HoCl_3$	6.46	2.1	6.9	2.5	6

Table S3: Electrochemical impedance spectroscopy (EIS) fitting parameters of the γ-$CsPbI_{2.5}Br_{0.5}$ and 3 % $HoCl_3$-based IPVSCs.

Perovskites films	**R*s* (Ω)**	$\mathbf{R_{rec}}$ **(Ω)**
γ-$CsPbI_{2.5}Br_{0.5}$	53	1352
3 % $HoCl_3$	93	1788

- **TRPL measurement details**

The obtained TRPL lifetime parameters were well fitted with a tri-exponential decay function from equation S1 [S5].

$$I(t) = I_0 + A_1 \exp\left(-\frac{t-t_0}{\tau_1}\right) + A_2 \exp\left(\frac{-t-t_0}{\tau_2}\right) + A_3 \exp\left(\frac{-t-t_0}{\tau_3}\right) \quad -- (S1)$$

Where, τ_1, τ_2 and τ_3 are first, second and third order decay time, A_1, A_2 and A_3 are respective weight factors of each decay channel. Here, τ_1 stands for the fast decay lifetime and τ_2 and τ_3 stand for the slow decay function. The average lifetimes $<\tau_{avg}>$ of γ-$CsPbI_{2.5}Br_{0.5}$ and 3 % $HoCl_3$-based perovskite thin films calculated from equation S2 [S6].

$$< \tau_{avg} >= \sum_n \frac{\Sigma A_n \tau_n^2}{\Sigma_m A_m \tau_m^2} \quad -- (S2)$$

- **V_{OC} as a function of illumination intensity**

The ideality factor (η) yielded by the slope of the fitted data, which was calculated by equations S3 and S4 [S6].

$$V_{OC} = nkT \ln(I)/q + A \quad \text{------- (S3)}$$

Where, k = Boltzmann constant, T = the temperature in Kelvin, q = the elementary charge and A is a constant according to the Shockley−Read−Hall (SRH) recombination mechanism [S7]. Equation S3 can be simplified for η as,

$$\eta = \text{slope} \times \frac{q}{kT} \quad \text{------- (S4)}$$

References:

[S1] J. V. Patil, S. S. Mali and C. K. Hong*, Sol. RRL*, 2020, 2000164.

[S2] S. S. Mali, J. V. Patil, J. A. Steele, S. R. Rondiya, N. Y. Dzade and C. K. Hong, *ACS Energy Lett*., 2021, **6,** 788.

[S3] S. S. Mali, J. V. Patil J. A. Steele and C. K. Hong, *Nano Energy,* 2021, **90,** 106597.

[S4] J. V. Patil, S. S. Mali and C. K. Hong, *J. Energy Chem.,* 2021, **62,** 458.

[S5] S. S. Mali, J. V. Patil, H. J. Kim and C. K. Hong, *Matter,* 2019, **1,** 464.

[S6] C. G. Shuttle, B. O. Regan, A. M. Ballantyne, J. Nelson, D. D. Bradley and J. R. Durrant, *Phys. Rev. B: Condens. Matter Mater. Phys.,* 2008, **78,** 113201.

[S7] H. Wang, J. H. Hsu, G. Yang and C. Yu, *Adv. Mater.,* 2016, **28,** 9545–9549.